Photoswitching the Efficacy of a Small-Molecule Ligand for a Peptidergic GPCR

Gómez-Santacana, Xavier; de Munnik, Sabrina M.; Vijayachandran, Prashanna; Da Costa Pereira, Daniel; Bebelman, Jan Paul M.; de Esch, Iwan J.P.; Vischer, Henry F.; Wijtmans, Maikel; Leurs, Rob

published in
Angewandte Chemie. International Edition
2018

DOI (link to publisher)
10.1002/anie.201804875

document version
Publisher's PDF, also known as Version of record

Photopharmacology

International Edition: DOI: 10.1002/anie.201804875
German Edition: DOI: 10.1002/ange.201804875

Photoswitching the Efficacy of a Small-Molecule Ligand for a Peptidergic GPCR: from Antagonism to Agonism

Xavier Gómez-Santacana[+], Sabrina M. de Munnik[+], Prashanna Vijayachandran, Daniel Da Costa Pereira, Jan Paul M. Bebelman, Iwan J. P. de Esch, Henry F. Vischer, Maikel Wijtmans, and Rob Leurs**

Abstract: *For optical control of GPCR function, we set out to develop small-molecule ligands with photoswitchable efficacy in which both configurations bind the target protein but exert distinct pharmacological effects, that is, stimulate or antagonize GPCR activation. Our design was based on a previously identified efficacy hotspot for the peptidergic chemokine receptor CXCR3 and resulted in the synthesis and characterization of five new azobenzene-containing CXCR3 ligands. G protein activation assays and real-time electrophysiology experiments demonstrated photoswitching from antagonism to partial agonism and even to full agonism (compound VUF16216). SAR evaluation suggests that the size and electron-donating properties of the substituents on the inner aromatic ring are important for the efficacy photoswitching. These compounds are the first GPCR azo ligands with a nearly full efficacy photoswitch and may become valuable pharmacological tools for the optical control of peptidergic GPCR signaling.*

Photopharmacology is an emerging discipline that involves the dynamic regulation of protein activity with light. Amongst others, freely diffusible photoswitchable ligands are used to regulate protein activity in a non-invasive and reversible manner with high spatiotemporal precision.[1] A commonly used strategy is to incorporate an azobenzene moiety into an existing bioactive ligand (azologization[1a]) to enable isomerization from a planar *trans* configuration to a bent *cis* configuration in response to near-ultraviolet light. Longer wavelengths or thermal relaxation can revert this photoisomerization, thus offering a dynamic approach to modulate ligand geometry. These geometrical changes can alter the binding affinity and/or efficacy of the ligand for its target protein.

In view of their important role in numerous (patho)physiological processes and high therapeutic relevance, G protein-coupled receptors (GPCRs) represent an excellent protein class for the development of photoswitchable ligands.[2] Recently, several photoswitchable ligands have been reported for GPCRs,[3] with some examples involving in vivo use.[4] Although it is not always straightforward to discern contributions by affinity or potency shifting from the contribution by any efficacy shift, most reported photoswitchable GPCR ligands display light-induced alterations in affinity or potency. We present herein the detailed photochemical and biochemical characterization of a class of photoswitchable ligands, the efficacy of which for a peptidergic G protein-coupled receptor can be controlled with light from antagonism to partial and, unprecedentedly, to full agonism.

To develop this proof of concept in GPCRs, we selected chemokine receptor CXCR3, which belongs to the class A GPCRs and is of interest because it plays a key role in T-cell function and CXCR3 agonism can aid in tissue repair.[5] CXCR3 signals through $G\alpha_i$ proteins in response to the endogenous agonist peptide ligands CXCL9, CXCL10, and CXCL11.[6] However, small-molecule CXCR3 agonists are scarce and limited to peptidomimetic ligands[7] and non-peptidomimetic biaryl-type ligands.[8] Structure–activity relationship studies on the latter revealed that increasing the size of a halogen substituent at the *ortho* position of the outer aryl ring increases the agonist efficacy, while shifting it to the *meta*

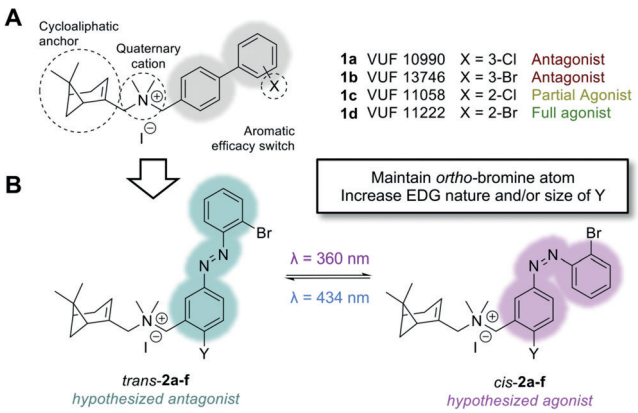

Figure 1. General design strategy. A) Examples of biaryl CXCR3 ligands that show differences in efficacy based on the position and size of a halogen substituent. B) Azologization of the scaffold of the biaryl CXCR3 ligands with the *ortho*-Br atom maintained and tailored Y groups to give photoisomerizable analogues of **1a–d** (i.e. **2a–f**). Illumination at 360 nm enables a switch from the *trans* to the *cis* configuration, and illumination at 434 nm reverts the photoisomerization. EDG = electron-donating group.

[*] Dr. X. Gómez-Santacana,[+] Dr. S. M. de Munnik,[+] P. Vijayachandran, D. Da Costa Pereira, J. P. M. Bebelman, Prof. Dr. I. J. P. de Esch, Dr. H. F. Vischer, Dr. M. Wijtmans, Prof. Dr. R. Leurs
Division of Medicinal Chemistry, Amsterdam Institute for Molecules, Medicines and Systems (AIMMS), Vrije Universiteit Amsterdam
De Boelelaan 1108, 1081 HZ, Amsterdam (The Netherlands)
E-mail: m.wijtmans@vu.nl
r.leurs@vu.nl

[+] These authors contributed equally.

Supporting information and the ORCID identification number(s) for the author(s) of this article can be found under: https://doi.org/10.1002/anie.201804875.

position yields antagonists (Figure 1 A).[8] Quantitative structure–activity relationships suggested that the electron density, a possible halogen bond, and/or geometrical differences as a result of the biaryl dihedral angle contribute to the agonist efficacies.[8] In the current study, we aimed to mimic this molecular efficacy hotspot by azologization of the biaryl moiety and as such enable optical control over the efficacy of the CXCR3 ligands.

A series of azobenzene-containing ligands was synthesized by replacing the biaryl moiety of **1a–d** with an azobenzene moiety to obtain **2a–f** (see Scheme S1 in the Supporting Information). The geometrical differences between *trans* and *cis* azobenzene isomers were hypothesized to be able to mimic the spatial changes of the biaryl moiety in **1a–d**. In all cases, the bromine atom at the *ortho* position of the outer aromatic ring was maintained to accommodate a potential halogen bond that was suggested to be important for the agonism of the parent biaryl ligands.[8] To explore the contribution of a possible conformational lock and electron density in the azobenzene moiety to the targeted efficacy switch, the substituent at the *para* position of the inner aromatic ring (Y, Figure 1 B and Table 1) was varied. To that end, halogen atoms of different sizes and electronegativity (F, Cl, and Br) and two different electron-donating groups (-OMe, -NMe_2) were used. On the basis of spatial considerations, agonism was hypothesized to reside in the *cis* isomer of these designed compounds.

First, the photochemical properties of **2a–f** were investigated by recording the UV/Vis absorption spectra after illumination (Table 1). In the dark, the *trans* isomers were identified (Table 1 and Figure 2 A; see also Figure S1 in the Supporting Information). Depending on the electron-donating properties of the Y substituent (Table 1), a slight redshift in the wavelengths of maximal absorbance of the π–π* band was observed. Upon illumination with 360 nm light, mainly the *cis* isomers of **2a–e** were observed (Figure 2 A; see also Figure S1 A–D), showing suitable photostationary states (PSSs) containing 89–93 % *cis* isomer (Table 1). After subsequent illumination of the samples with 434 nm light, mostly *trans* isomers of **2a–e** were detected (Figure 2 A; see also Figure S1 A–D). Unfortunately, **2f** decomposed under 360 nm illumination (see Figure S1 E) and was therefore omitted from further pharmacological characterization. Photoisomerization of **2e** was confirmed by ^{1}H NMR (Figure 2 C) and LC–MS (Figure 2 D) analysis. In both LC–MS and NMR analysis, only *trans*-**2e** was observed in the dark, whereas a PSS of 95 % *cis*-**2e** after 360 nm illumination and a PSS of 75 % *trans*-**2e** after 434 nm back-illumination were identified (in [D_6]DMSO). Compound **2e** displayed high resistance toward photochemical wear (Figure 2 E), and the long relaxation half-lives of *cis*-**2a–e** indicate the bistable nature of **2a–e** (Figure 2 B, Table 1; see also Figure S2).

Compounds **2a–e** were tested for their ability to bind to CXCR3. Control **1a** inhibited [^{125}I]CXCL10 binding to membranes prepared from CXCR3-expressing cells with a pIC_{50} value of 6.4 ± 0.1, a result comparable to previous findings.[8] Compounds **2a–e** were tested in the dark (corresponding to > 99 % *trans* isomer) and at the PSS after illumination for 15 min with 360 nm light. Owing to the bistable nature of **2a–e**, the photostationary state was assumed to remain unaltered after illumination during the assay time. All *trans* isomers of **2a–e** inhibited [^{125}I]CXCL10 binding in a concentration-dependent manner with similar submicromolar IC_{50} values (Table 1 and Figure 3 A). On the contrary, after illumination to the PSS, **2a–e** demonstrated pIC_{50} values increasing with enhanced size and electron-donating properties of substituent Y (Table 1 and Figure 3 A). For example, **2a** showed no photoinduced affinity shift (PAS) upon illumination, whereas **2e** displayed the largest PAS with an eightfold higher pIC_{50} value at the PSS than that of its *trans* form (Table 1).

A [^{35}S]GTPγS functional binding assay was used to measure the intrinsic activity (α) as a means to quantify the efficacy of these photoswitchable ligands. As CXCL11 has the highest potency and efficacy of all three endogenous ligands for CXCR3,[9] it was deemed the best chemokine control for functional assays. Control **1d** (VUF11222) acts as a full agonist, as compared to CXCL11 (see Figure S3 A,B), as was previously

Table 1: Photoisomerization properties and binding affinities of **2a–f** for human CXCR3. Percentage of photoisomerization, pIC_{50} values, and photoinduced affinity switches are shown as the mean ± standard error of the mean (SEM) of at least three independent experiments, each performed in triplicate.

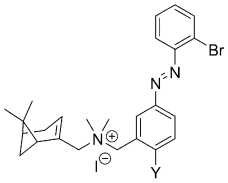

Cpd.	Y	Photoisomerization *trans* λ_{max}[a] [nm]	*cis* λ_{max}[a] [nm]	PSS[b] [%]	$t_{1/2}$[c] [days]	[^{125}I]CXCL10 binding[d] pIC_{50} *trans*	pIC_{50} at PSS	PAS[e]
2a	H	325	420	88.9 ± 0.4	109	6.0 ± 0.1	6.0 ± 0.1	1.0 ± 0.1
2b	F	327	420	92.7 ± 0.1	92	6.0 ± 0.0	6.2 ± 0.0	1.6 ± 0.0
2c	Cl	331	419	92.6 ± 0.2	55	5.9 ± 0.1	6.2 ± 0.1	2.0 ± 0.4
2d	Br	334	424	92.6 ± 0.2	61	5.8 ± 0.1	6.4 ± 0.1	3.8 ± 0.4
2e	OMe	353	428	92.1 ± 0.1	29	5.9 ± 0.0	6.8 ± 0.0	8.3 ± 1.3
2f	NMe_2	387	dec.[f]	dec.[f]	dec.[f]			

[a] The absorbance maxima were extracted from UV/Vis spectra (10 μM in HEPES buffer with 1 % DMSO at 25 °C, Figure 2 A, Figure S1). [b] The photostationary state (PSS) was measured as the percentage area of the *cis* isomer as compared to the combined areas of *cis* and *trans* isomers as detected by LC at 265 nm. Samples were 1 mM in 68 vol % TRIS buffer and 32 vol % DMSO. [c] The thermal relaxation half-life was determined by allowing a PSS sample (10 μM in HEPES buffer with 1 % DMSO) to thermally isomerize at 25 °C in the dark (see Figure S2). [d] The pIC_{50} value was measured by [^{125}I]CXCL10 binding experiments using membranes prepared from HEK293T cells expressing CXCR3. [e] The photoinduced affinity switch (PAS) was calculated as the ratio of the IC_{50} value of the *trans* isomer and that corresponding to the PSS. [f] dec. = decomposition under illumination at 360 nm.

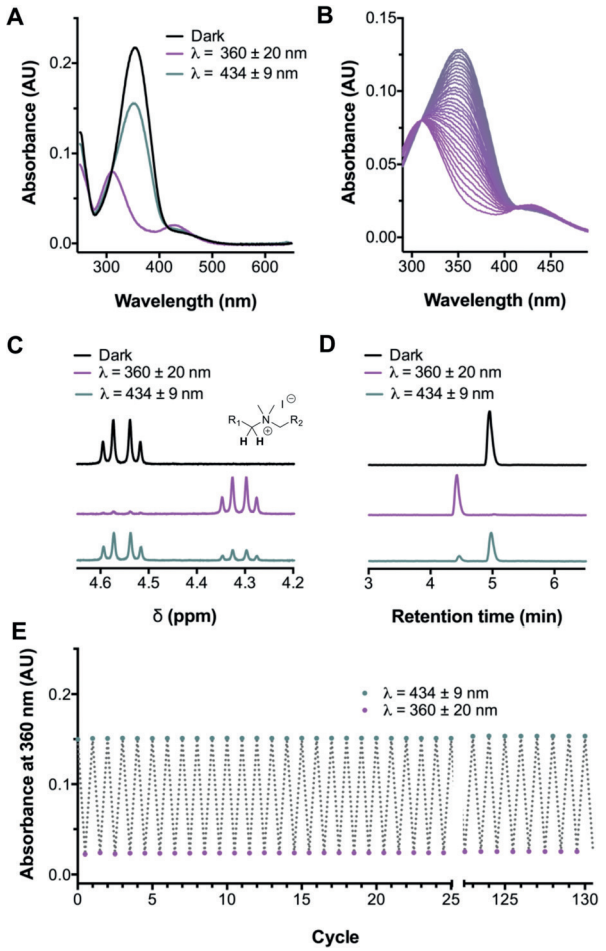

Figure 2. Photochemical properties of **2e**. A) UV/Vis absorption spectra of 10 μM **2e** in HEPES buffer with 1% DMSO at 25 °C under dark conditions (black), after illumination with 360 nm light for 2 min (magenta), and after back-illumination for 2 min with 434 nm light (turquoise). B) UV/Vis absorption spectra of 10 μM **2e** in HEPES buffer after attainment of the PSS, measured every 24 h for 30 days at 25 °C. C,D) Isomerization of 1 mM **2e** in [D_6]DMSO as analyzed by ^{1}H NMR spectroscopy (C; α-ammonium methylene hydrogen atoms with signals at 4.56 and 4.31 ppm for the *trans* and *cis* isomers, respectively) and LC–MS analysis (D). E) UV/Vis absorption measurements of 10 μM **2e** in HEPES buffer at 360 nm after repeated cycles of illumination with 360 (magenta) and 434 nm light (turquoise). DMSO = dimethyl sulfoxide.

reported.[8] We did not observe any alteration of potency or efficacy of **1d** as a result of illumination (Table 2; see Figure S3B). All *trans* compounds **2a–e** acted as antagonists or very weak partial agonists with low efficacies (Figure 3C and Table 2; see also Figure S3C–F). On the other hand, **2a–d** illuminated to the PSS acted as partial agonists with comparable submicromolar potencies (Table 2; see also Figure S3C–F). The efficacy of **2a–d** at the PSS qualitatively correlates with the size and the electron-donating properties of the *para* substituent (Y) of the inner aromatic ring (Figure 3B and Table 2). Confirming this trend, **2e** at the PSS acted as a full agonist ($\alpha = 0.99$; Table 2 and Figure 3C) and consequently showed the largest photoinduced difference of efficacy (PDE; Table 2).

To address the possibility of nonspecific effects on the receptor activity as a result of compound microprecipitation,[10] we performed nephelometry experiments (see Figure S5),[11] which revealed no microprecipitation of *trans*-**2a–e** or *cis*-**2a–e** at pharmacologically relevant concentrations.

The full agonism of **2e** at the PSS can possibly be explained by the size of the -OMe group in the Y position and/or the more significant electron-donating properties as compared to halogen substituents. Unfortunately, this potential explanation could not be further explored with a -NMe_2 moiety owing to the chemical instability of **2f** under illumination. We observed a correlation between PDE and PAS values ($r = 0.986$, $P = 0.0024$; see Figure S4). This correlation is probably a result of more efficient inhibition of [^{125}I]CXCL10 binding by photoisomers with higher efficacy through preferential binding to a subset of CXCR3 conformations that overlap with those preferentially binding the endogenous agonist CXCL10.[12]

The photoinduced efficacy switch of **2e** was evaluated dynamically in real-time electrophysiology measurements using the two-electrode voltage clamp (TEVC) technique in *Xenopus laevis* oocytes transiently coexpressing CXCR3 and G protein-coupled inwardly rectifying potassium (GIRK) channels. Control agonist **1d** induced GIRK channel activation, which was not affected by several illumination cycles with 360 and 434 nm light, and the initial current was restored upon washing out with a buffer (not shown). GIRK channels were not activated by *trans*-**2e** (Figure 3D), as expected for an antagonist/weak partial agonist, but a slight outward current was observed. Indeed, it is well known that quaternary ammonium ions may interact with GIRK channels[13] or other potassium channels.[14] Illumination of the perfused oocytes expressing CXCR3 and GIRK with 360 nm light prompted the photoisomerization of *trans*-**2e** to the *cis* configuration and consequently induced the activation of CXCR3, leading to GIRK channel activation (Figure 3D) and thus confirming CXCR3 agonism of **2e** at the PSS in the oocyte expression system. This effect could be reverted by 434 nm illumination, and repeated cycles of illumination with 360 and 434 nm light clearly showed the reversible activation of CXCR3 by photoswitching *trans*-**2e** to its *cis* isomer and vice versa (Figure 3D). The antagonist behavior of *trans*-**2e** was confirmed by competition with agonist **1d** in the same CXCR3-expressing oocyte system (Figure 3E). In the dark, *trans*-**2e** antagonized the CXCR3 activation induced by **1d**, and this effect was reverted upon illumination with 360 nm light. Subsequent illumination with 434 nm light recovered the antagonism of *trans*-**2e.**

Taken together, we have demonstrated optical control of CXCR3 activity by photoswitching small-molecule antagonists/weak partial agonists to agonists with different efficacies up to full agonism. The isomerization from the *trans* to the *cis* configuration was designed to probe a very subtle efficacy hotspot that was identified in earlier studies. Real-time electrophysiology measurements confirmed the reversibility of an efficacy switch from antagonism to agonism during several illumination cycles. These compounds, particularly **2e**, will be excellent tools for elucidating CXCR3 signaling owing to the distinctive spatiotemporal control of functional activity

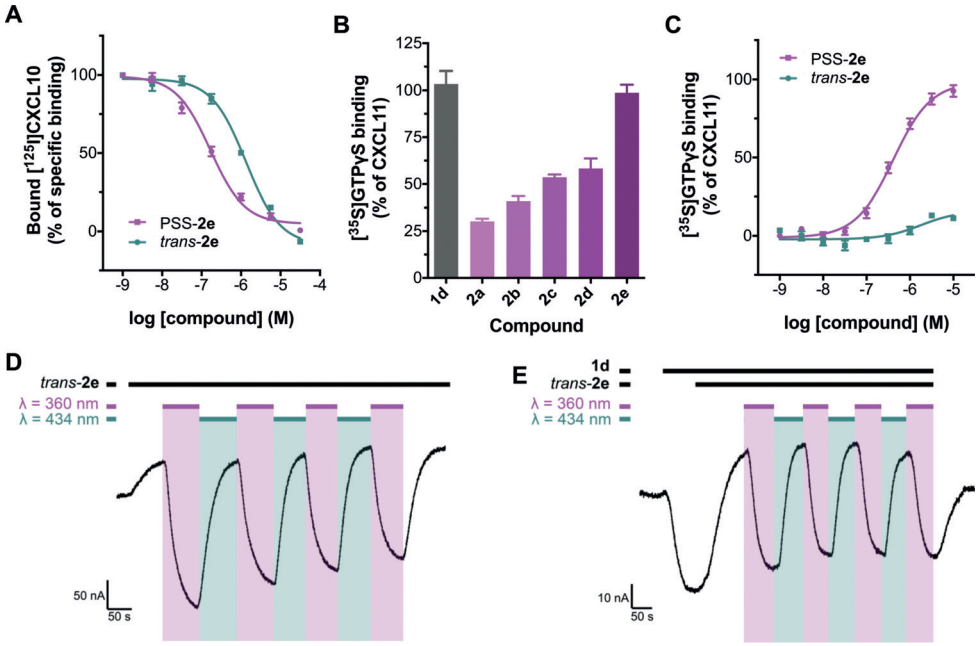

Figure 3. Pharmacological characterization of **2a–e**. A) Binding experiments with [^{125}I]CXCL10 were performed in the presence of increasing concentrations of **2e** in the dark (turquoise) or at the PSS after illumination at 360 nm (magenta) using membranes prepared from HEK293T cells expressing human CXCR3. B,C) Maximum responses (efficacy) of **1d** and **2a–e** after illumination at 360 nm (B) and concentration–response curves of *trans*-**2e** and **2e** at the PSS (C), as determined in a [^{35}S]GTPγS binding experiment using membranes prepared from HEK293T cells expressing human CXCR3. Data are presented as the percentage of specific [^{125}I]CXCL10 binding (A) or as the percentage of the maximum response induced by the endogenous agonist CXCL11 (B,C) and represent the mean ± SEM from at least three independent experiments, each performed in triplicate (A) or duplicate (B,C). D,E) Representative traces of two-electrode voltage clamp experiments in *X. laevis* oocytes expressing human CXCR3 and GIRK in the presence of **2e** (10 μM; D) or **2e** (10 μM) in competition with **1d** (1 μM; E) with 360 (magenta) and 434 nm light (turquoise) illumination cycles (concentrations in high-potassium solution with 0.1% DMSO).

Table 2: Efficacy and potency of **2a–e** and control **1d** as determined by [^{35}S]GTPγS binding experiments using membranes prepared from HEK293T cells expressing human CXCR3. Potency, intrinsic activity, and values for PDE are shown as the mean ± SEM of three independent experiments, each performed in duplicate.

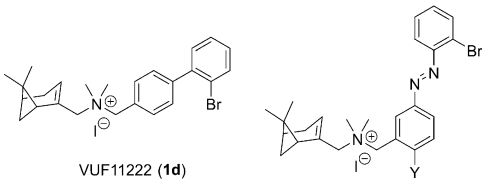

Cpd.	Y	α[a] *trans*	α[a] at PSS	PDE[b]	pEC_{50} *trans*	pEC_{50} at PSS
1d	–	1.04 ± 0.08	1.03 ± 0.07	0.00 ± 0.03	6.9 ± 0.0	6.9 ± 0.0
2a	H	0.05 ± 0.03	0.30 ± 0.01	0.25 ± 0.02	–[c]	6.5 ± 0.1
2b	F	0.12 ± 0.00	0.41 ± 0.03	0.30 ± 0.03	–[c]	6.2 ± 0.1
2c	Cl	0.11 ± 0.01	0.54 ± 0.01	0.42 ± 0.01	–[c]	6.3 ± 0.1
2d	Br	0.14 ± 0.02	0.58 ± 0.05	0.45 ± 0.04	–[c]	6.2 ± 0.1
2e	OMe	0.16 ± 0.01	0.99 ± 0.04	0.83 ± 0.06	–[c]	6.4 ± 0.1

[a] The ligand intrinsic activity (α) was determined relative to the maximum response of the endogenous full agonist CXCL11 (for which α is set to 1.0). [b] The photoinduced difference of efficacy (PDE) was obtained by subtracting the intrinsic activity under dark conditions from the intrinsic activity at PSS. [c] Could not be determined, as the efficacy and/or potency was too low.

provided by light. Such photocontrol may also be of interest for topical treatments, such as wound healing, in which CXCR3 agonism plays a key role.[5] Further efforts will be undertaken to understand the mechanism of action of these compounds and improve their biocompatibility (e.g. redshifting photoisomerization wavelengths).[15] To our knowledge, **2a–e** are the first small-molecule synthetic GPCR ligands that harbor a rationally designed efficacy photoswitch. Moreover, **2e** (VUF16216) represents the highest photoinduced efficacy switch for a GPCR azo-ligand reported to date and provides a real-time efficacy switch from antagonism to agonism. Our results together with other reported GPCR efficacy photoswitchers may contribute to the development of a second generation of photoswitchable ligands with light-dependent functional activity switches.

Acknowledgements

We acknowledge the Netherlands Organisation for Scientific Research for financial support (TOPPUNT, "7 ways to 7TMR modulation (7-to-7)", 718.014.002). We thank Danny Scholten, Chris de Graaf, Shanliang Sun, and Luc Roumen for helpful discussions, Hans Custers for recording HRMS spectra, and Mounir Andaloussi for providing **4**.

Conflict of interest

The authors declare no conflict of interest.

Keywords: azo compounds · efficacy photoswitching · G protein-coupled receptors · photochromism · photopharmacology

How to cite: *Angew. Chem. Int. Ed.* **2018**, *57*, 11608–11612
Angew. Chem. **2018**, *130*, 11782–11786

[1] a) J. Broichhagen, J. A. Frank, D. Trauner, *Acc. Chem. Res.* **2015**, *48*, 1947–1960; b) M. M. Lerch, M. J. Hansen, G. M. van Dam, W. Szymanski, B. L. Feringa, *Angew. Chem. Int. Ed.* **2016**, *55*, 10978–10999; *Angew. Chem.* **2016**, *128*, 11140–11163; c) A. A. Beharry, G. A. Woolley, *Chem. Soc. Rev.* **2011**, *40*, 4422–4437.

[2] A. S. Hauser, M. M. Attwood, M. Rask-Andersen, H. B. Schioth, D. E. Gloriam, *Nat. Rev. Drug Discovery* **2017**, *16*, 829–842.

[3] a) M. Schönberger, D. Trauner, *Angew. Chem. Int. Ed.* **2014**, *53*, 3264–3267; *Angew. Chem.* **2014**, *126*, 3329–3332; b) S. Pittolo, X. Gomez-Santacana, K. Eckelt, X. Rovira, J. Dalton, C. Goudet, J. P. Pin, A. Llobet, J. Giraldo, A. Llebaria, P. Gorostiza, *Nat. Chem. Biol.* **2014**, *10*, 813–815; c) M. I. Bahamonde, J. Taura, S. Paoletta, A. A. Gakh, S. Chakraborty, J. Hernando, V. Fernandez-Duenas, K. A. Jacobson, P. Gorostiza, F. Ciruela, *Bioconjugate Chem.* **2014**, *25*, 1847–1854; d) J. Broichhagen, N. R. Johnston, Y. von Ohlen, H. Meyer-Berg, B. J. Jones, S. R. Bloom, G. A. Rutter, D. Trauner, D. J. Hodson, *Angew. Chem. Int. Ed.* **2016**, *55*, 5865–5868; *Angew. Chem.* **2016**, *128*, 5961–5965; e) L. Agnetta, M. Kauk, M. C. A. Canizal, R. Messerer, U. Holzgrabe, C. Hoffmann, M. Decker, *Angew. Chem. Int. Ed.* **2017**, *56*, 7282–7287; *Angew. Chem.* **2017**, *129*, 7388–7393; f) M. V. Westphal, M. A. Schafroth, R. C. Sarott, M. A. Imhof, C. P. Bold, P. Leippe, A. Dhopeshwarkar, J. M. Grandner, V. Katritch, K. Mackie, D. Trauner, E. M. Carreira, J. A. Frank, *J. Am. Chem. Soc.* **2017**, *139*, 18206–18212; g) N. J. Hauwert, T. A. M. Mocking, D. Da Costa Pereira, A. J. Kooistra, L. M. Wijnen, G. Vreeker, N. W. E. Verweij, B. H. De Boer, M. J. Smit, C. de Graaf, H. F. Vischer, I. J. P. De Esch, M. Wijtmans, R. Leurs, *J. Am. Chem. Soc.* **2018**, *140*, 4232–4243.

[4] a) M. H. Berry, A. Holt, J. Levitz, J. Broichhagen, B. M. Gaub, M. Visel, C. Stanley, K. Aghi, Y. J. Kim, K. Cao, R. H. Kramer, D. Trauner, J. Flannery, E. Y. Isacoff, *Nat. Commun.* **2017**, *8*, 1862; b) X. Gómez-Santacana, S. Pittolo, X. Rovira, M. Lopez, C. Zussy, J. A. Dalton, A. Faucherre, C. Jopling, J. P. Pin, F. Ciruela, C. Goudet, J. Giraldo, P. Gorostiza, A. Llebaria, *ACS Cent. Sci.* **2017**, *3*, 81–91; c) C. Zussy, X. Gomez-Santacana, X. Rovira, D. De Bundel, S. Ferrazzo, D. Bosch, D. Asede, F. Malhaire, F. Acher, J. Giraldo, E. Valjent, I. Ehrlich, F. Ferraguti, J. P. Pin, A. Llebaria, C. Goudet, *Mol. Psychiatry* **2018**, *23*, 509–520.

[5] A. C. Huen, A. Wells, *Adv. Wound Care (New Rochelle)* **2012**, *1*, 244–248.

[6] J. R. Groom, A. D. Luster, *Exp. Cell Res.* **2011**, *317*, 620–631.

[7] M. Wijtmans, D. Scholten, W. Mooij, M. J. Smit, I. J. P. de Esch, C. de Graaf, R. Leurs in *Chemokines: Chemokines and Their Receptors in Drug Discovery* (Ed.: N. Tschammer), Springer International Publishing, Cham, **2015**, pp. 119–185.

[8] M. Wijtmans, D. J. Scholten, L. Roumen, M. Canals, H. Custers, M. Glas, M. C. Vreeker, F. J. de Kanter, C. de Graaf, M. J. Smit, I. J. de Esch, R. Leurs, *J. Med. Chem.* **2012**, *55*, 10572–10583.

[9] C. E. Heise, A. Pahuja, S. C. Hudson, M. S. Mistry, A. L. Putnam, M. M. Gross, P. A. Gottlieb, W. S. Wade, M. Kiankarimi, D. Schwarz, P. Crowe, A. Zlotnik, D. G. Alleva, *J. Pharmacol. Exp. Ther.* **2005**, *313*, 1263–1271.

[10] M. F. Sassano, A. K. Doak, B. L. Roth, B. K. Shoichet, *J. Med. Chem.* **2013**, *56*, 2406–2414.

[11] K. A. Dehring, H. L. Workman, K. D. Miller, A. Mandagere, S. K. Poole, *J. Pharm. Biomed. Anal.* **2004**, *36*, 447–456.

[12] M. A. Cox, C. H. Jenh, W. Gonsiorek, J. Fine, S. K. Narula, P. J. Zavodny, R. W. Hipkin, *Mol. Pharmacol.* **2001**, *59*, 707–715.

[13] R. Andrade, *Eur. J. Pharmacol.* **1991**, *199*, 259–262.

[14] M. Zhou, J. H. Morais-Cabral, S. Mann, R. MacKinnon, *Nature* **2001**, *411*, 657–661.

[15] a) M. Dong, A. Babalhavaeji, S. Samanta, A. A. Beharry, G. A. Woolley, *Acc. Chem. Res.* **2015**, *48*, 2662–2670; b) D. Bléger, S. Hecht, *Angew. Chem. Int. Ed.* **2015**, *54*, 11338–11349; *Angew. Chem.* **2015**, *127*, 11494–11506.

Manuscript received: April 30, 2018
Accepted manuscript online: June 21, 2018
Version of record online: August 6, 2018

